Effect of the Inner-Zone Vibrations on the Dynamics of Collision-Induced Intramolecular Energy Flow in Highly Excited Toluene

Jongbaik Ree,[*] Yoo Hang Kim,[†] and Hyung Kyu Shin[‡]

Department of Chemistry Education, Chonnam National University, Gwangju 500-757, Korea. [*]E-mail: jbree@chonnam.ac.kr
[†]Department of Chemistry and Center for Chemical Dynamics, Inha University, Incheon 402-751, Korea
[‡]Department of Chemistry, University of Nevada, Reno, Nevada 89557, U.S.A.
Received April 25, 2005

Key Words : Inner-zone, Collision-induced, Intramolecular, Toluene, Ar

The dynamics of intramolecular energy transfer of large molecules has been the subject of a great deal of attention from both experimentalists and theorists.[1-11] In recent years, collisions involving large molecules have been studied actively, revealing valuable information on the rates and the mechanism of vibrational energy transfer processes. The average energy transfer per collision between the vibrationally highly excited benzene and a noble gas atom is known to be about −30 cm^{-1}, which is much smaller than benzene derivatives such as hexafluorobenzene and other hydrocarbons such as toluene and azulene.[4,5,12-15] For example, the mean energy transfer per collision measured by the ultraviolet absorption method for hexafluorobenzene + Ar, is −330 cm^{-1},[14] whereas the calculated value for the same system at 300 K using quasiclassical trajectory methods is −150 cm^{-1}.[5] For toluene + Ar, the amount of energy transfer is about −200 cm^{-1}.[15] These magnitudes are much larger than the results for benzene colliding with argon. Among large organic molecules, toluene is a particularly attractive molecule for the study of collision-induced intramolecular energy flow because of the presence of both methyl and ring CH bonds, presenting an intriguing competition between them. In elucidating this competition, it is particularly important to understand the direction of intramolecular energy flow in the interaction zone, *i.e.*, from the ring CH to the methyl CH or the reverse.

In this paper, an extension of the previous works in refs. 10 and 11, we study the collision-induced dynamics of vibrationally highly excited methyl CH bond or the ring CH bond of toluene interacting with argon using quasiclassical trajectory calculations with particular emphasis on the effect of the inner zone on the energy transfer which was not included in our previous works.[11] Using the solutions of the equations of motion, we discuss the collision-induced energy transfer in the Ar-toluene system and intramolecular energy transfers among various stretches and bends of toluene, especially their time evolution. We then analyze the nature and mechanism of the competition in transferring energy to or from the incident atom and between the methyl CH mode and the ring CH mode. We set the initial vibrational energy of the highly excited methyl CH bond or the ring CH bond equal to the state just 0.10 eV below the dissociation threshold of each bond at 300 K.

Interaction Model

The present work follows the interaction model and numerical procedure which have already been reported in ref. 10 except the fact that the inner zone vibrations are

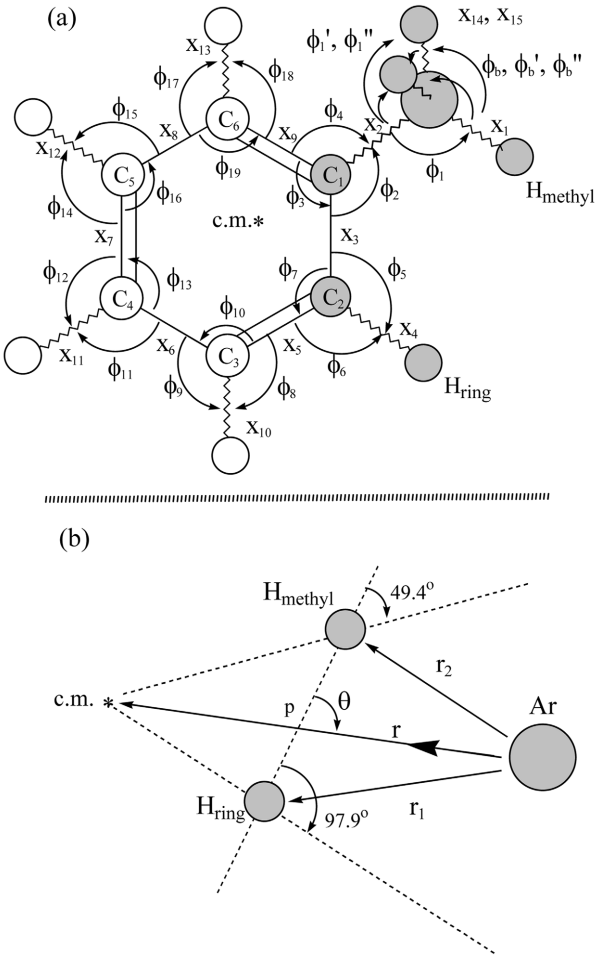

Figure 1. Collision model. (a) The stretching and bending coordinates of vibrations included in the model. All carbon atoms and ring H atoms are coplanar and modes are numbered clockwise. The star denotes the position of the center-of-mass (c. m.) of toluene. (b) The relative coordinate between Ar and the c. m. of toluene (r), the Ar-to-H_{ring} distance (r_1) and the Ar-to-H_{methyl} distance (r_2) are shown.

explicitly included in the present work. Briefly, we recapitulate the essential aspects of the interaction of Ar with toluene, reproducing the collision model in Figure 1 for easy reference. We define the interaction model and geometric parameters of toluene for the toluene-Ar interaction in Figure 1, where all carbon atoms, the ring hydrogen atoms and the incident atom are assumed to be coplanar. In Figure 1a, we define all 39 intermolecular coordinates of the planar ring needed to be included in the present study. In Figure 1b, we define the interaction coordinates between the methyl CH bond and the adjacent ring CH bond of a non-rotating toluene with the incident argon atom. The CH_{ring} bond is in the clockwise side from CH_{methyl}. The modes between these two bonds (designated by the x_1 and x_4 stretches, respectively) are the C-CH_{methyl} stretch, the $(CC)_{ring}$ stretch, the CCH_{methyl} bend, the CCC_{methyl} bend and the CCH_{ring} bend, which are denoted in Figure 1a as x_2, x_3, ϕ_1, ϕ_2 and ϕ_5, respectively. Here $(CC)_{ring}$ is the benzene ring's CC bond linking the methyl group and the H_{ring} atom. These modes and other ring modes are identified in the clockwise order in Figure 1a. Two other CCH bends of the methyl side are ϕ_1' and ϕ_1'' and two other CH stretches are x_{14} and x_{15}. The HCH bends of the methyl group are ϕ_b, ϕ_b', and ϕ_b''. Other bends around the C_1 carbon atom are designated by ϕ_3 and ϕ_4. Similarly, the two other bends around the C_2 carbon atom are ϕ_6 and ϕ_7. We include all these modes (6 stretches and 12 bends) in the interaction zone where the CH_{methyl} and CH_{ring} bonds are in direct interaction with Ar. We then include the x_5-x_9 $(CC)_{ring}$ stretches, x_{10}-x_{13} $(CH)_{ring}$ stretches and ϕ_8-ϕ_{19} bends around the carbon atoms C_3, C_4, C_5 and C_6, the total of 9 stretches and 12 bends, in the inner zone of the molecule.

The overall interaction energy is assumed as the sum of the Morse-type intermolecular terms, Morse-type stretching terms, the harmonic bending terms, and intramolecular coupling terms. All potential and spectroscopic constants needed in the calculation are listed in ref. 10. In our earlier work, we already showed that the interaction near $\theta = 77°$ plays the dominant role in promoting energy loss through intramolecular energy redistribution.[9] In all collision systems considered here, thus, we consider that the incident atom approaches the center of mass of toluene in the $\theta = 77°$ direction, where the Ar-CH_{methyl} and Ar-CH_{ring} interactions are very close to each other and where energy transfer is most efficient.

Numerical Procedures

We solve the equations of motion for the relative motion, 15 stretches and 24 bends using the DIVPAG double-precision routine of the IMSL library[16,17] to describe the time evolution of bond distances, angles, and vibrational energies, as well as the relative coordinate for the model system. We sample 40,000 trajectories for each run at 300 K, where the sampling includes determining collision energies (E) chosen from the Maxwell distribution.[9,18] The initial conditions for solving the equations of motion for the relative motion and the displacements and phases for the vibrational motions in the interaction zone are given in ref. 9. We introduce the desired initial vibrational energy, which is 0.10 eV below the dissociation threshold for both CH_{ring} and CH_{methyl} stretches. All the other vibrations are assumed to have the zero-point energy.

The conditions for the vibrational motions in the inner zone take the same forms. Each vibrational phase is a random number $\delta_i = 2\pi s_i$ with flat distribution of s_i in the interval (0,1). The initial separation between the center of mass of toluene and Ar is set as 15 Å, and trajectories are terminated when the separation reaches 50 Å after they passed through the closest distance of approach. The integration was performed with a step size of 0.169 fs, which is one-tenth of the period of the largest frequency, the ring CH vibration, and is small enough to ensure energy conservation to at least five significant figures along the entire trajectory.

Since the dissociation energies are 3.9717 eV and 4.9569 eV for the CH_{methyl} and CH_{ring} bonds, respectively, the initial vibrational energy content for the highly excited CH_{methyl} is $D_{CHmethyl}$-0.1000 eV = 3.8717 eV or 31,230 cm^{-1} and that for the highly excited CH_{ring} bond is D_{CHring}-0.1000 eV = 4.8569 eV or 39,170 cm^{-1} above the bottom of the potential well. Note that these two energies reduce to 29,700 cm^{-1} and 37,600 cm^{-1}, respectively, when we take the initial vibrational energies above the zero-point. The initial energy content of the molecule, E_T, is defined in terms of these energies. We will consider two systems of different initial vibrational energies. In system (i) we set the CH_{methyl} to be in the highly excited state and all other vibrations in the ground state, *i.e.*, E_T = 29,700 cm^{-1}. In system (ii), the CH_{ring} stretch is now in the highly excited state, whereas all others are in the ground state, *i.e.*, E_T = 37,600 cm^{-1}.

We define the ensemble-averaged energy transfer $\langle\Delta E\rangle = \langle E_{final}\text{-}E\rangle$, the difference between the final and initial total vibrational energy of toluene. Thus, a negative value of $\langle\Delta E\rangle$ represents the ensemble-averaged energy loss by toluene, a V $\rightarrow$ T energy transfer process. We also determine the ensemble average of vibrational energy of each mode consisting of kinetic and potential energy terms, and then calculate the difference between this average energy and the energy initially deposited in the mode.

Results and Discussion

A. Energy Transfer. In system (i), $\langle\Delta E\rangle$ is −24 cm^{-1} for nondissociative trajectories, which are 39,356 out of the total of 40,000 sampled. Here, a negative value of the ensemble-averaged energy transfer indicates that the molecule loses energy to Ar, *i.e.*, the deexcitation of CH_{methyl} *via* a V $\rightarrow$ T pathway. In system (ii), where all trajectories are non-reactive, the ensemble-averaged energy transfer is $\langle\Delta E\rangle$ = 116 cm^{-1} or 0.0144 eV, which represents a gain of energy by the molecule (T $\rightarrow$ V energy transfer), but the gain is not enough to cause the CH_{ring} bond dissociation. In nonreactive collisions, these results indicate that toluene with its highly excited CH_{ring} bond tends to be further excited, whereas the

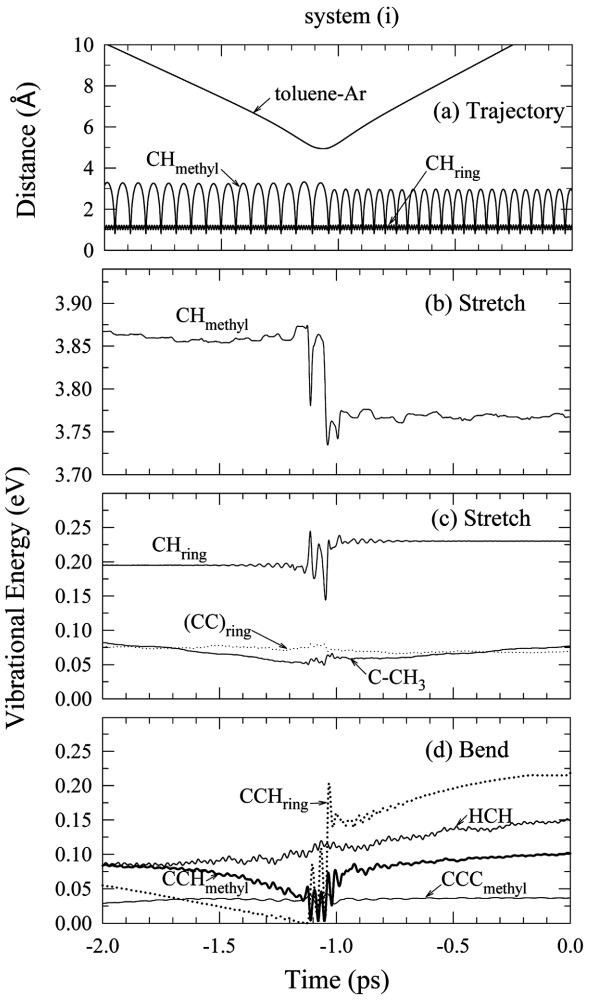

Figure 2. Time evolution of the collision trajectory, bond trajectories and energies representing the nondissociative events for the highly excited CH_{methyl}, System (i). (a) Toluene-Ar collision and CH_{methyl} and CH_{ring} bond trajectories. (b) The vibrational energy of the highly excited CH_{methyl} stretch in the interaction zone. (c) The vibrational energies of the ground state CH_{ring}, $(CC)_{ring}$ and $C\text{-}CH_3$ stretches. (d) The vibrational energies of the ground state CCH_{methyl}, HCH, CCC_{methyl} and CCH_{ring} bends. The CCH_{methyl} curve is shown by a heavy line for easy reference.

molecule with the highly excited CH_{methyl} bond tends to relax.

Now we look into the details of energy transfer characteristics for several representative cases, in particular, time evolution of the collision trajectories and energy flow events. In Figure 2, we show the time evolution of a collision event representing a typical nondissociative trajectory of system (i). For this representative event, a sharp decrease in the CH_{methyl} (x_1) vibrational energy over a short period shown in Figure 2b indicates that the essential part of relaxation of the highly excited CH_{methyl} bond is over within 0.2 ps, which is much shorter than the duration of collision. The amount of energy transferred from CH_{methyl} to other modes during this short period is nearly 0.11 eV, which is far greater than the thermal energy k_BT at 300 K. Transfer of such a large amount of energy in molecular collisions represents the occurrence of strong collisions.[5] This is both interesting and important in studying molecular collision processes, since such a short-time scale for large amounts of energy transfer means that the processes of deactivation (or activation shown below for CH_{ring}) occur essentially in single-step processes as opposed to ladder-climbing processes in which bonds gain or lose their energy in a series of small steps. The occurrence of such stepwise processes has been noted in classical trajectory calculations of collision-induced intramolecular energy flow in the OC···Ni···CO complex.[19] As shown in Figure 2c, the CH_{ring} bond at the other end of the interaction zone gains about 0.03 eV during a slightly longer period than the 0.2 ps time scale given above for the vibrational relaxation of CH_{methyl}, but it is still a short-time process. The main reservoir of energy is the ϕ_5 CCH_{ring} bend, see Figure 2d. Also, the HCH bend of the methyl group gains some energy. However, all other modes shown in Figures 2c and 2d change their initial vibrational energy contents only slightly after collision.

The time evolution of the collision event representing system (ii) is shown in Figure 3. The principal feature of the curves shown in this figure is the inefficiency of intramolecular energy flow processes, especially to or from the highly excited CH_{ring} bond, compared to the previous case shown in Figure 2. For all modes considered in Figures 3b, 3c and 3d, the initial vibrational energies, especially those of the stretching modes, change only slightly after collision. The time evolution of the highly excited CH_{ring} bond trajectory (Figure 3a) shows the bond becoming compressed while undergoing the collision, during which the CH_{ring} vibrational energy oscillates many times (Figure 3b). After many energy give-and-take steps, the amount of energy eventually lost by the highly excited CH_{ring} bond when the collision is over is only 0.0054 eV or 44 cm^{-1}. Thus, unlike the highly excited CH_{methyl} case, the CH_{ring} bond gains or lose energy in a series of small steps, which leads to the amount of energy transfer very small compared to k_BT.

We now consider Ar interacting with either the highly excited CH_{ring} bond or the ground-state CH_{methyl} bond, which is a modification of system (ii). Either situation leads to further excitation of the CH_{ring} vibration, which is consistent with the result presented above for the simultaneous interaction of Ar with both CH_{methyl} and CH_{ring}, system (ii). The values of energy transfer in this modified system $\langle\Delta E\rangle$ = 104 cm^{-1} when Ar interacts with the CH_{methyl} end and $\langle\Delta E\rangle$ = 136 cm^{-1} when Ar interacts with the CH_{ring} end, both being close to $\langle\Delta E\rangle$ = 116 cm^{-1} when Ar interacts with both CH_{methyl} and CH_{ring}. In all these cases, therefore, the excitation is not large enough to cause the dissociation of the highly excited CH_{ring} bond. However, if the mechanism of energy flow to the inner zone is absent (*i.e.*, the *restricted* model described in ref. 10), the interaction of Ar *only* with the ground-state CH_{methyl} end leads to the dissociation of the highly excited ring CH at the other end of the interaction zone because of energy flow from CH_{methyl}.[10]

B. Energy Propagation into the Inner Zone. The problem of energy transfer to the stretches and bends in the

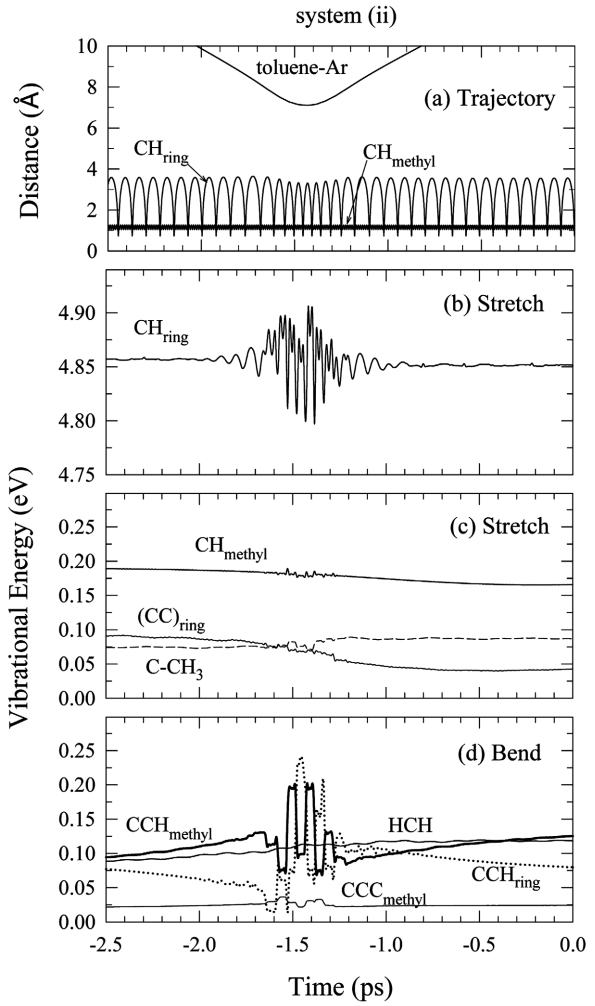

Figure 3. Time evolution of the collision trajectory, bond trajectories and energies representing the nondissociative events for the highly excited CH_{ring}, System (ii). (a) Toluene-Ar collision and CH_{ring} and CH_{methyl} bond trajectories. (b) The vibrational energy of the highly excited CH_{ring} stretch in the interaction zone. (c) The vibrational energies of the ground state CH_{methyl}, $(CC)_{ring}$ and C-CH_3 stretches. (d) The vibrational energies of the ground state CCH_{methyl}, HCH, CCH_{ring} and CCC_{methyl} bends. The CCH_{methyl} curve is shown in a heavy line for easy reference.

inner zone of toluene is complicated largely because of the coupling of numerous modes in both inner and interaction zones. Although this complication makes a systematic discussion of energy flow from the interaction zone to the inner zone difficult, we can still discover several important aspects in the present study. One result which stands out in both systems (i) and (ii) is the extreme difficulty of energy transfer to the inner ring CH stretching vibrations (x_{10}, x_{11}, x_{12} and x_{13} modes), the amount of energy transfer being on the order of 10^{-5} eV, which is negligible compared with E_T or $3/2k_BT$. In system (i), most of the energy coming from the highly excited CH_{methyl} bond and the incident atom rapidly passes through the bending modes around C_1 and then through the x_3 $(CC)_{ring}$ stretch in the "clockwise" direction. The energy then deposits in the ϕ_5 CCH_{ring} bending mode of the interaction zone. This directional preference is due to the model where Ar interacts with the methyl CH bond and the adjacent ring CH, which is the position in the clockwise side from CH_{methyl}. The vibrational modes around CH_{ring} then become labile due to the perturbation caused by the interaction with Ar, thus making energy flow easy compared to the modes adjacent to C_6, where the CH bond is not in a direct interaction with Ar (see Figure 1b). Further propagation of energy from the ϕ_5 mode to the ϕ_8 and ϕ_{12} CCH bends takes place without depositing energy in the intermediate modes, x_5 $(CC)_{ring}$ stretch and the bends around C_2, C_3 and C_4. We find the deposit of a noticeable amount of energy in the x_6 $(CC)_{ring}$ stretch.

In the bending modes around each carbon in system (i), one of the three modes receives energy, while another loses energy. The remaining bend does not change its energy appreciably, suggesting the energies of these three bends redistribute among themselves without receiving much from the interaction zone. For example, in the three bends around C_3, ϕ_8 gains energy while ϕ_9 loses, but the energy of ϕ_{10} is nearly unchanged. Although it is not large, the x_6 $(CC)_{ring}$ stretch between C_3 and C_4 receives the most energy in the inner zone. A similar trend is found in system (ii), but the magnitudes of energy deposited in these modes are much less than those in system (i).

In the "counter-clockwise" direction in system (i), energy from CH_{methyl} propagates to the ϕ_{17} CCH bend and then the x_8 and x_7 $(CC)_{ring}$ stretches, and the ϕ_{14} bend as well. However, the magnitudes of energy transfer in this direction are much less than those in the "clockwise" direction. Although the individual energy varies as noted above, the three bends around each carbon atom are strongly coupled to each other and the sum of their energies does not change greatly. As a result, energy propagated into the bends in the inner zone from Ar-CH_{methyl} interaction site is not large, but the bending modes are generally more effective in gaining energy that is propagated from the interaction zone than most of the stretching modes because the coupling force constants of the bending modes are larger than those of the most of the stretching modes.[20] Among the bending modes around C_6, as the bends around C_3 noted above, the ϕ_{17} mode gains energy and ϕ_{18} loses, whereas the energy of ϕ_{19} changes only slightly. The amounts of energy propagated to the x_7 and x_9 $(CC)_{ring}$ stretches are very small. Although it is close to the Ar-CH_{methyl} interaction site, the x_9 $(CC)_{ring}$ stretch is perturbed less compared to the x_3 stretch and gains only a small amount of energy.

In a nonreactive case, only small portion of the energy initially stored in CH_{methyl} or CH_{ring}, in addition to the energy from the incident atom transfers to the modes in the inner zone. In the interaction zone, the energy deposits mainly in the bending modes as noted in systems (i) and (ii). The portion of the energy that has propagated into the inner zone deposits in various modes as displayed in Figure 4b. For easy reference we define the numbering sequence in the clockwise direction from the interaction zone as in Figure 4a. The three bending modes around C_3, namely ϕ_8, ϕ_9 and ϕ_{10} are grouped together and numbered as 2. Similarly

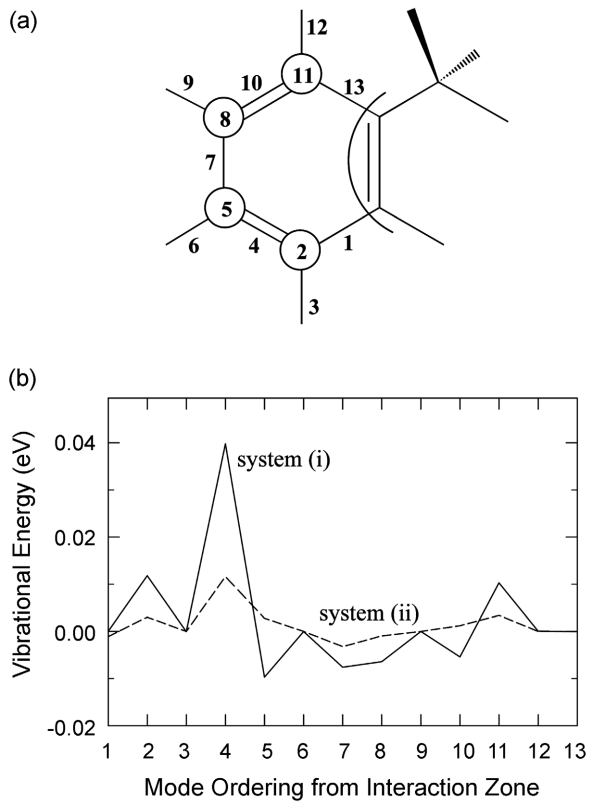

Figure 4. (a) Ordering of the vibrational modes in the inner zone used in (b). (b) Vibrational energy transfer to the inner zone modes for the representative trajectories of Systems (i) and (ii) using the ordering shown in (a).

grouped are (ϕ_{11}, ϕ_{12}, ϕ_{13}) as 5, (ϕ_{14}, ϕ_{15}, ϕ_{16}) as 8 and (ϕ_{17}, ϕ_{18}, ϕ_{19}) as 11. Such grouping of energies for the coupled bends is physically reasonable in interpreting a set of strongly coupled modes as their energies continue to redistribute among them. Most of the energy transferred to the inner zone for system (i) deposits in the bends around C_3 and the ring x_6 $(CC)_{ring}$ stretch. There is some deposit in the bends around C_6, where the energy comes from the Ar-CH_{methyl} interaction through the x_9 $(CC)_{ring}$ stretch, but energy propagation in this direction on the ring is much less efficient compared to the propagation in the other direction as noted above. The general characteristic of energy flow along the ring in Figure 4a is that the amount of energy flow becomes very small as the mode gets farther removed from the interaction zone. For system (ii) the trend is the same except that the amount is much smaller. The magnitude and the time scale of energy flow from the CH_{methyl}-Ar and CH_{ring}-Ar collisions to various stretches and bends in the inner zone as well as those in the interaction zone indicate that energy transfer to the inner zone is irreversible.[9]

Acknowledgments. The authors gratefully acknowledge the financial support from 2005 Inha University research grant. Part of the computational time was provided by the 6th Supercomputing Application Supporting Program of the Korea Institute of Science and Technology Information.

References

1. Lim, K. F. *J. Chem. Phys.* **1994**, *101*, 8756.
2. Wright, S. M. A.; Sims, I. R.; Smith, I. W. M. *J. Phys. Chem. A* **2000**, *104*, 10347.
3. Hippler, H.; Troe, J. In *Bimolecular Collisions*; Ashfold, M. N. R.; Baggott, J. E., Eds.; Royal Society of Chemistry: London, 1989.
4. Toselli, B. M.; Barker, J. R. *J. Chem. Phys.* **1992**, *97*, 1809.
5. Lenzer, T.; Luther, K.; Troe, J.; Gilbert, R. G.; Lim, K. F. *J. Chem. Phys.* **1995**, *103*, 626.
6. Bernshtein, V.; Lim, K. F.; Oref, I. *J. Phys. Chem.* **1995**, *99*, 4531.
7. Clary, D. C.; Gilbert, R. G.; Bernshtein, V.; Oref, I. *Faraday Discuss.* **1995**, *102*, 423.
8. Shin, H. K. *J. Phys. Chem. A* **2000**, *104*, 6699.
9. Ree, J.; Kim, Y. H.; Shin, H. K. *J. Chem. Phys.* **2002**, *116*, 4858.
10. Ree, J.; Kim, Y. H.; Shin, H. K. *Chem. Phys. Lett.* **2004**, *394*, 250.
11. Ree, J.; Chang, K. S.; Kim, Y. H.; Shin, H. K. *Bull. Korean Chem. Soc.* **2003**, *24*, 1223.
12. Hippler, H.; Troe, J.; Wendelken, H. J. *J. Chem. Phys.* **1983**, *78*, 6709.
13. Yerram, M. L.; Brenner, J. D.; King, K. D.; Barker, J. R. *J. Phys. Chem.* **1990**, *94*, 6341.
14. Damm, M.; Hippler, H.; Olschewski, H. A.; Troe, J.; Willner, J. *Z. Phys. Chem. N.F.* **1990**, *166*, 129.
15. Toselli, B. M.; Brenner, J. D.; Yerram, M. L.; Chin, W. E.; King, K. D.; Barker, J. R. *J. Chem. Phys.* **1991**, *95*, 176.
16. Gear, C. W. *Numerical Initial Value Problems in Ordinary Differential Equations*; Prentice-Hall: New York, 1971.
17. MATH/LIBRARY *Fortran Subroutines for Mathematical Applications*; IMSL: Houston, 1989; p 640.
18. Ko, Y.; Ree, J.; Kim, Y. H.; Shin, H. K. *Bull. Korean Chem. Soc.* **2002**, *23*, 1737.
19. Shin, H. K. *J. Phys. Chem.* **1990**, *94*, 598.
20. Guan, Y.; Thompson, D. L. *J. Chem. Phys.* **1990**, *92*, 313.